Contemporary Mathematics
https://ojs.wiserpub.com/index.php/CM/

Research Article

Solitary Wave Structures Under Stochastic Influence in a Nonlinear Optical System Governed by an Augmented Fokas-Lenells Equation

Ahmed Ramady[1,2], Hamdy M. Ahmed[3*], Khadiga A. Ismail[4], Wafaa B. Rabie[5]

[1] GRC Department, The Applied College, King Abdulaziz University, Jeddah, 21589, Saudi Arabia
[2] Department of Mathematics and Computer Science, Faculty of Science, Beni-Suef University, Beni-Suef, Egypt
[3] Department of Physics and Engineering Mathematics, Higher Institute of Engineering, El Shorouk Academy, Cairo, Egypt
[4] Department of Clinical Laboratory Sciences, College of Applied Medical Sciences, Taif University, Taif, 21944, Saudi Arabia
[5] Department of Basic Sciences, Higher Institute of Engineering and Technology, Menoufia, Egypt
E-mail: hamdy_17eg@yahoo.com

Received: 1 July 2025; **Revised:** 23 July 2025; **Accepted:** 31 July 2025

Abstract: This paper investigates the stochastic dynamics of optical solitons in the Fokas-Lenells equation, incorporating nonlinear chromatic dispersion and generalized quadratic-cubic Self-Phase Modulation (SPM). As a non-trivial extension of the Nonlinear Schrödinger Equation (NLSE), the Fokas-Lenells framework accurately models ultrashort pulse propagation in optical fibers where higher-order nonlinearities and complex dispersion effects dominate. We employ the Modified Extended Mapping Method (MEMM) to derive comprehensive analytical solutions under stochastic perturbations that realistically represent noise in fiber-optic systems. Our approach yields multiple solution classes, including dark and singular solutions, exponential-type solutions, periodic wave solutions (both trigonometric and elliptic), Jacobi elliptic function solutions, Weierstrass elliptic solutions, and hyperbolic function solutions. The MEMM proves particularly effective in handling the mathematical complexity of the stochastic NLSE class of equations, maintaining solution integrity while accommodating physical constraints. Through systematic parametric analysis, we identify critical condition regimes where each solution type emerges, providing new insights into noise-resistant soliton propagation in advanced photonic systems.

***Keywords*:** stochastic wave pattern, generalized Fokas-Lenells optical model, generalized self-phase modulation, modified extended mapping scheme

MSC: 35C05, 35R60, 35C07, 35C08, 35C09

1. Introduction

Optical solitons, stable, localized waves that maintain their shape through a precise balance between dispersion and nonlinearity, have revolutionized modern photonics [1–5]. First predicted theoretically by Hasegawa and Tappert in 1973 [6], these robust wave packets defy conventional pulse degradation, enabling high-capacity optical communication and ultrafast laser technologies [7, 8]. Their unique ability to preserve energy and shape over long distances arises from a dynamic equilibrium: temporal dispersion broadens the pulse, while intensity-dependent nonlinearity counteracts this spread via self-focusing [6, 7]. The Nonlinear Schrödinger Equation (NLSE) serves as the cornerstone of soliton theory,

DOI: https://doi.org/10.37256/cm.6420257653

modeling wave propagation in dispersive nonlinear media [9–11]. However, the NLSE fails to capture femtosecond pulse dynamics or exotic waveguides (e.g., photonic crystal fibers and metamaterials) [12, 13]. This limitation has spurred advanced frameworks like the Fokas-Lenells Equation (FLE), an integrable generalization of the NLSE incorporating nonlinear chromatic dispersion [14]. The FLE is pivotal for modeling ultrashort pulses in media with higher-order dispersion, wave dynamics in $X^{(2)} - X^{(3)}$ nonlinear systems (e.g., periodically poled lithium niobate), and plasmonic platforms [15, 16]. Recent extensions of the FLE include generalized quadratic-cubic Self-Phase Modulation (SPM), combining Kerr (cubic) and parametric (quadratic) effects [17, 18]. Despite its theoretical promise, the interplay between nonlinear dispersion and quadratic-cubic SPM remains underexplored, particularly in stochastic regimes [19, 20]. Real-world systems face perturbations—thermal noise, material inhomogeneities, and amplifier-induced stochasticity—that can destabilize solitons or trigger collapse phenomena [21, 22]. A stochastic FLE framework is thus essential for applications in noise-resilient optical communications, frequency comb generation, and topological photonic circuits [23, 24]. Parallel advances in control theory, such as [25, 26], demonstrate the critical role of adaptive mechanisms in managing nonlinear stochastic systems, offering insights for optical soliton stabilization. This work investigates the stochastic dynamics of FLE solitons with nonlinear dispersion and quadratic-cubic SPM, governed by [27]:

$$\begin{aligned} &i\mathscr{F}_t + \alpha(\mathscr{F}|\mathscr{F}|^n)_{xx} + \left(\beta_1|\mathscr{F}|^m + \beta_2|\mathscr{F}|^{2m}\right)\mathscr{F} + i\eta\mathscr{F}_x|\mathscr{F}|^2 \\ &- i\left[\beta_3\mathscr{F}_x + \delta\mathscr{F}(|\mathscr{F}|^2)_x + \lambda(\mathscr{F}|\mathscr{F}|^2)_x\right] + \sigma_1\mathscr{F}\frac{dw(t)}{dt} = 0, \end{aligned} \tag{1}$$

where $\mathscr{F}(x, t)$ is the complex-valued optical wave envelope; α is the nonlinear chromatic dispersion coefficient; β_1 and β_2 denote quadratic and cubic SPM coefficients, respectively; η represents nonlinear dispersion; β_3, δ, and λ account for intermodal dispersion, self-frequency shifts, and self-steepening; and $\sigma_1\frac{dw(t)}{dt}$ models white noise (Wiener process derivative) [27, 28]. Recent studies of deterministic Fokas-Lenells Equation (FLE) systems have established crucial foundations for optical soliton analysis. However, these works exhibit significant limitations in addressing realistic stochastic effects prevalent in practical optical communication systems. Prior deterministic studies include [28], who derived dark and anti-dark solitons for FLE with damping perturbations using inverse scattering methods, but restricted to idealized constant dispersion conditions. Three fundamental gaps persist in the current literature: a lack of generalized frameworks combining nonlinear chromatic dispersion with quadratic-cubic SPM, oversimplification of noise models (primarily additive noise while ignoring multiplicative effects), and limited analytical methods capable of handling coupled nonlinearities in stochastic regimes. This work bridges these critical gaps through three key innovations: a Modified Extended Mapping Method (MEMM) framework resolving FLE with nonlinear chromatic dispersion and quadratic-cubic SPM under both additive and multiplicative noise, first exact stochastic soliton solutions incorporating realistic fiber imperfections (thermal fluctuations, amplifier noise), and a demonstration of noise-induced soliton stability thresholds beyond previous deterministic predictions. The proposed MEMM approach overcomes limitations of traditional methods (e.g., Kudryashov's or Riccati techniques) through a unified treatment of coupled nonlinearities and stochastic terms, exact solutions preserving phase-space topology, and explicit noise-soliton interaction terms absent in prior studies. Compared to existing integro-differential approaches [4, 29], our framework provides closed-form solutions rather than numerical approximation, direct physical interpretation of noise parameters, and experimentally verifiable stability criteria. This research is organized into four main sections. Section 2 presents the MEMM formulation for stochastic FLE. Section 3 presents exact soliton solutions with nonlinear dispersion. Section 4 presents graphical validation of stochastic soliton profiles. Section 5 presents the conclusion.

2. Algorithm of modified extended mapping method

In this section, we present the fundamental computational framework of the Modified Extended Mapping Method (MEMM). This systematic approach enables the derivation of exact analytical solutions for Nonlinear Partial Differential Equations (NLPDEs). The method proceeds through the following key stages [29, 30]:

Step 1: Consider a Nonlinear Partial Differential Equation (NLPDE) expressed as:

$$\mathscr{G}(\mathscr{F}, \mathscr{F}_t, \mathscr{F}_x, \mathscr{F}_{tt}, \mathscr{F}_{xx}, \ldots\ldots) = 0, \tag{2}$$

where $\mathscr{G}$ is a polynomial function of the unknown function $\mathscr{F}(x,t)$ and its partial derivatives, with $\mathscr{F}$ being the dependent variable of the independent variables x and t.

Step 2: We utilize the traveling wave transformation to obtain solutions as follows:

$$\mathscr{F}(x,t) = \mathscr{P}(\zeta), \qquad \zeta = \mathscr{K}\, x + \sigma_1\, t, \tag{3}$$

where $\mathscr{K}$ represents the wave number (spatial frequency) and σ_1 denotes the temporal frequency. Applying this transformation to Eq. (3) yields the nonlinear ODE:

$$\mathscr{H}(\mathscr{P}, \mathscr{P}', \mathscr{P}'', \ldots\ldots) = 0. \tag{4}$$

Step 3: The proposed solution to Eq. (4) is supposed to be in the following form:

$$\mathscr{P}(\xi) = \sum_{j=0}^{N} \mathscr{A}_j\, \mathscr{V}^j(\zeta) + \sum_{j=2}^{N} \frac{\mathscr{B}_{-j}\, \mathscr{V}'(\zeta)}{\mathscr{V}^{2-j}(\zeta)} + \sum_{j=-1}^{-N} \frac{\mathscr{C}_{-j}\, \mathscr{V}'(\zeta)}{\mathscr{V}^{-j}(\zeta)} + \sum_{j=-1}^{-N} \frac{\mathscr{D}_{-j}}{\mathscr{V}^{-j}(\zeta)}, \tag{5}$$

where $\mathscr{A}_j$, $\mathscr{B}_{-j}$, $\mathscr{C}_{-j}$ and $\mathscr{D}_{-j}$ are constants, $\mathscr{V}$ is a function that satisfies the following:

$$\mathscr{V}' = \sqrt{\rho_0 + \rho_1\, \mathscr{V} + \rho_2\, \mathscr{V}^2 + \rho_3\, \mathscr{V}^3 + \rho_4\, \mathscr{V}^4 + \rho_6\, \mathscr{V}^6}. \tag{6}$$

Real-valued constants are represented by ρ_i $(i = 0, 1, 2, 3, 4, 6)$. This equation provides many basic solutions from which additional exact solutions for Eq. (4) can be obtained.

Step 4: We determine the integer N by balancing the highest-order linear and nonlinear terms in Eq. (4).

Step 5: The selection of distinct parameter combinations for ρ_0, ρ_1, ρ_2, ρ_3, ρ_4, ρ_6 in Eq. (6) yields multiple exact solution classes, as demonstrated in the following analysis:

Case 1: When $\rho_0 = \rho_1 = \rho_3 = \rho_6 = 0$,

$$\mathscr{V}(\zeta) = \sqrt{-\frac{\rho_2}{\rho_4}}\ \operatorname{sech}\left[\zeta\ \sqrt{\rho_2}\right], \quad \rho_2 > 0, \quad \rho_4 < 0.$$

$$\mathscr{V}(\zeta) = \sqrt{-\frac{\rho_2}{\rho_4}}\ \sec\left[\zeta\ \sqrt{-\rho_2}\right], \quad \rho_2 < 0, \quad \rho_4 > 0.$$

$$\mathscr{V}(\zeta) = \sqrt{-\frac{\rho_2}{\rho_4}}\ \csc\left[\zeta\ \sqrt{-\rho_2}\right], \quad \rho_2 < 0,\ \ \rho_4 > 0.$$

Case 2: When $\rho_1 = \rho_3 = \rho_6 = 0$, $\rho_0 = \dfrac{\rho_2^2}{4\,\rho_4}$,

$$\mathscr{V}(\zeta) = \sqrt{-\frac{\rho_2}{2\,\rho_4}}\ \tanh\left[\zeta\ \sqrt{-\frac{\rho_2}{2}}\right], \quad \rho_2 < 0,\ \ \rho_4 > 0.$$

$$\mathscr{V}(\zeta) = \sqrt{\frac{\rho_2}{2\,\rho_4}}\ \tan\left[\zeta\ \sqrt{\frac{\rho_2}{2}}\right], \quad \rho_2 > 0,\ \ \rho_4 > 0.$$

Case 3: When $\rho_3 = \rho_4 = \rho_6 = 0$,

$$\mathscr{V}(\zeta) = \frac{\rho_1}{2\,\rho_2}\ \sinh\left[2\ \zeta\ \sqrt{\rho_2}\right] - \frac{\rho_1}{2\rho_2}, \ \ \rho_2 > 0,\ \ \rho_0 = 0.$$

$$\mathscr{V}(\zeta) = \frac{\rho_1}{2\,\rho_2}\ \sin\left[2\ \zeta\ \sqrt{-\rho_2}\right] - \frac{\rho_1}{2\rho_2}, \ \ \rho_2 < 0,\ \ \rho_0 = 0.$$

$$\mathscr{V}(\zeta) = \sqrt{\frac{\rho_0}{\rho_2}}\ \sinh\left[\zeta\sqrt{\rho_2}\right], \ \ \rho_0 > 0,\ \ \rho_2 > 0,\ \ \rho_1 = 0.$$

$$\mathscr{V}(\zeta) = \sqrt{-\frac{\rho_0}{\rho_2}}\ \sin\left[\zeta\ \sqrt{-\rho_2}\right], \ \ \rho_0 > 0,\ \ \rho_2 < 0,\ \ \rho_1 = 0.$$

$$\mathscr{V}(\zeta) = \exp\left[\zeta\ \sqrt{\rho_2}\right] - \frac{\rho_1}{2\rho_2}, \ \ \rho_2 > 0,\ \ \rho_0 = \frac{\rho_1^2}{4\rho_2}.$$

Case 4: When $\rho_0 = \rho_1 = \rho_6 = 0$,

$$\mathscr{V}(\zeta) = -\frac{\rho_2}{\rho_3}\ \left(\tanh\left[\frac{1}{2}\ \zeta\ \sqrt{\rho_2}\right] + 1\right), \quad \rho_3^2 = 4\ \rho_2\ \rho_4, \ \ \rho_2 > 0.$$

$$\mathscr{V}(\zeta) = -\frac{\rho_2}{\rho_3}\ \left(\coth\left[\frac{1}{2}\ \zeta\ \sqrt{\rho_2}\right] + 1\right), \quad \rho_3^2 = 4\ \rho_2\ \rho_4, \ \ \rho_2 > 0.$$

$$\mathscr{V}(\zeta) = \frac{\rho_2\ \operatorname{sech}^2\left[\dfrac{1}{2}\ \zeta\ \sqrt{\rho_2}\right]}{2\ \sqrt{\rho_2\ \rho_4}\ \tanh\left[\dfrac{1}{2}\ \zeta\ \sqrt{\rho_2}\right] - \rho_3}, \quad \rho_3^2 \neq 4\rho_2\rho_4, \ \ \rho_2 > 0, \ \ \rho_4 > 0.$$

$$\mathscr{V}(\zeta) = -\frac{\rho_2 \ \sec^2\left[\frac{1}{2}\ \zeta\ \sqrt{-\rho_2}\right]}{2\ \sqrt{-\rho_2\ \rho_4}\ \tan\left[\frac{1}{2}\ \zeta\ \sqrt{-\rho_2}\right] - \rho_3}, \quad \rho_3^2 \neq 4\rho_2\rho_4, \quad \rho_2 < 0, \quad \rho_4 > 0.$$

Case 5: When $\rho_2 = \rho_4 = \rho_6 = 0$,

$$\mathscr{V}(\zeta) = \wp\left(\frac{1}{2}\ \zeta\ \sqrt{\rho_3}; -\frac{4\ \rho_1}{\rho_3}, -\frac{4\ \rho_0}{\rho_3}\right), \qquad \rho_3 > 0.$$

Case 6: When $\rho_1 = \rho_3 = 0$,

$$\mathscr{V}(\zeta) = \sqrt{\frac{2\ \rho_2\ \operatorname{sech}^2\left[\ \zeta\ \sqrt{\rho_2}\right]}{2\ \sqrt{\rho_4^2 - 4\ \rho_2\ \rho_6} - \left(\sqrt{\rho_4^2 - 4\ \rho_2\ \rho_6} + \rho_4\right)\operatorname{sech}^2\left[\ \zeta\ \sqrt{\rho_2}\right]}}, \qquad \rho_2 > 0.$$

$$\mathscr{V}(\zeta) = \sqrt{\frac{2\ \rho_2\ \sec^2\left[\ \zeta\ \sqrt{-\rho_2}\right]}{2\ \sqrt{\rho_4^2 - 4\ \rho_2\ \rho_6} - \left(\sqrt{\rho_4^2 - 4\ \rho_2\ \rho_6} + \rho_4\right)\sec^2\left[\ \zeta\ \sqrt{-\rho_2}\right]}}, \qquad \rho_2 < 0.$$

Step 6: Substituting Eq. (5) into Eq. (4), and using Eq. (6), yields a polynomial in ρ. Setting coefficients of like powers to zero generates a system of equations that can be solved using mathematical software to determine the unknown parameters $\mathscr{A}_j$, $\mathscr{B}_{-j}$, $\mathscr{C}_{-j}$, $\mathscr{D}_{-j}$, and ρ_i. This process provides exact solutions for Eq. (2).

3. Traveling wave solutions for Fokas-Lenells equation

To obtain precise solutions for Eq. (1), we utilize the MEMM approach. The following form is expected for the solutions:

$$\mathscr{F}(x, t) = \mathscr{P}(\zeta)\ e^{i\left(qt - \sigma_1^2 t + \sigma_1 w(t) + \vartheta\right)}, \tag{7}$$

and

$$\zeta = \mathscr{K}\ x, \tag{8}$$

Here, $\mathscr{P}(\zeta)$ represents the soliton amplitude, $\mathscr{K}$ is the wave vector, q denotes the frequency, and ϑ corresponds to the phase shift of the optical soliton. The parameter σ_1 quantifies the noise strength, and $w(t)$ describes a one-dimensional standard Wiener process.

We begin by applying the traveling wave transformation specified in Eq. (7) to the governing Eq. (1). Subsequent separation into real and imaginary components yields the following coupled equations:

$$\alpha\ \mathscr{K}^2\ (n+1)\ \mathscr{P}^{n+1}\ \mathscr{P}'' + \alpha\ \mathscr{K}^2\ n(n+1)\ \mathscr{P}^n\ \left(\mathscr{P}'\right)^2 + \beta_1\ \mathscr{P}^{m+2} + \beta_2\ \mathscr{P}^{2m+2} + \left(\sigma_1^2 - q\right)\mathscr{P}^2 = 0, \tag{9}$$

and

$$\mathscr{K}\ \left(\beta_3 + \mathscr{P}^2(2\ \delta - \eta + 3\ \lambda)\right)\ \mathscr{P}\ \mathscr{P}' = 0. \tag{10}$$

Let

$$\beta_3 = 0,\ \ m = n\ \ \&\ \ \eta = 2\delta + 3\lambda. \tag{11}$$

Consequently, Eq. (9) can be expressed in the following form:

$$\alpha\ \mathscr{K}^2\ (n+1)\ \mathscr{P}^{n+1}\ \mathscr{P}'' + \alpha\ \mathscr{K}^2\ n\ (n+1)\ \mathscr{P}^n\ \left(\mathscr{P}'\right)^2 + \beta_1\ \mathscr{P}^{n+2} + \beta_2\ \mathscr{P}^{2n+2} + \left(\sigma_1^2 - q\right)\ \mathscr{P}^2 = 0. \tag{12}$$

To simplify the preceding equation, we introduce the following assumption:

$$\mathscr{P} = \mathscr{H}^{\frac{2}{n}}. \tag{13}$$

Thus, Eq. (12) can be reformulated as:

$$2\alpha\ \mathscr{K}^2\ n(n+1)\ \mathscr{H}\ \mathscr{H}'' + 2\alpha\ \mathscr{K}^2\ (n+1)(n+2)\ \left(\mathscr{H}'\right)^2 + \beta_2\ n^2\ \mathscr{H}^4 + \beta_1\ n^2\ \mathscr{H}^2 + n^2\ \left(\sigma_1^2 - q\right) = 0. \tag{14}$$

To establish the solution structure, we apply the balance principle to Eq. (14), which determines $N = 1$. Accordingly, the solution form for $\mathscr{H}$ follows from Eq. (5) as:

$$\mathscr{H} = \mathscr{A}_0 + \mathscr{A}_1\ \mathscr{V}(\zeta) + \frac{\mathscr{C}_1\ \mathscr{V}'(\zeta)}{\mathscr{V}(\zeta)} + \frac{\mathscr{D}_1}{\mathscr{V}(\zeta)}, \tag{15}$$

The constants $\mathscr{A}_0$, $\mathscr{A}_1$, $\mathscr{C}_1$, and $\mathscr{D}_1$ are to be determined. Substituting $\mathscr{H}$ from Eq. (15) and incorporating Eq. (6) into Eq. (14), we collect coefficients of like powers of $\mathscr{V}^i$. Equating these coefficients to zero yields a system of algebraic equations, whose solution leads to the exact traveling wave solutions of Eq. (1).

Case Study 1: Assume that $\rho_0 = \rho_1 = \rho_3 = \rho_6 = 0$. The following solution set is obtained in this instance:

$$\mathscr{A}_0 = \mathscr{A}_1 = \mathscr{D}_1 = 0,\ \mathscr{C}_1 = \frac{4\mathscr{K}\ (n+1)\ \sqrt{2\alpha\ (n+1)\left(q - \sigma_1^2\right)}}{\beta_1\ n\ \sqrt{n+2}},\ \beta_2 = \frac{\beta_1^2\ (n+2)(3n+2)}{16(n+1)^2\left(\sigma_1^2 - q\right)},\ \rho_2 = \frac{\beta_1\ n^2}{8\alpha\ \mathscr{K}^2(n+1)^2}.$$

In this instance, these parameter restrictions result in the following physically relevant answers to Eq. (1):

(1.1) Under the parametric constraints $\beta_1 \mathscr{K} < 0$, $\alpha\left(q-\sigma_1^2\right) > 0$, $\rho_2 > 0$ and $\rho_4 < 0$, the system admits the following classes of solution:

$$\mathscr{F}_{1.1} = \left(-\frac{4\mathscr{K}(n+1)\sqrt{2\alpha\ (n+1)\ \rho_2\left(q-\sigma_1^2\right)}}{\beta_1\ n\ \sqrt{n+2}}\ \tanh\left[\mathscr{K}\ x\sqrt{\rho_2}\right] \right)^{\frac{2}{n}} e^{i\left(qt-\sigma_1^2 t+\sigma_1 w(t)+\vartheta\right)}, \tag{16}$$

this is known as a dark soliton solution.

(1.2) Under the parametric constraints $\alpha\left(q-\sigma_1^2\right) > 0$, $\rho_2 < 0$ and $\rho_4 > 0$, the system admits the following classes of solutions:

$$\mathscr{F}_{1.2} = \left(\frac{4\mathscr{K}(n+1)\sqrt{-2\alpha\ (n+1)\ \rho_2\left(q-\sigma_1^2\right)}}{\beta_1\ n\ \sqrt{n+2}}\ \tan\left[\mathscr{K}\ x\sqrt{-\rho_2}\right] \right)^{\frac{2}{n}} e^{i\left(qt-\sigma_1^2 t+\sigma_1 w(t)+\vartheta\right)},\ \beta_1\ \mathscr{K} > 0, \tag{17}$$

or

$$\mathscr{F}_{1.3} = \left(\frac{-4\mathscr{K}(n+1)\sqrt{-2\alpha\ (n+1)\ \rho_2\left(q-\sigma_1^2\right)}}{\beta_1\ n\ \sqrt{n+2}}\ \cot\left[\mathscr{K}\ x\sqrt{-\rho_2}\right] \right)^{\frac{2}{n}} e^{i\left(qt-\sigma_1^2 t+\sigma_1 w(t)+\vartheta\right)},\ \beta_1\ \mathscr{K} < 0, \tag{18}$$

these are known as singular periodic wave solutions.

Case Study 2: Assume that $\rho_0 = \dfrac{\rho_2^2}{4\rho_4}$, $\rho_1 = \rho_3 = \rho_6 = 0$. The following solution sets are obtained in this instance:

(2.1)

$$\mathscr{A}_0 = \mathscr{D}_1 = \mathscr{C}_1 = 0,\ \mathscr{A}_1 = \frac{4\mathscr{K}(n+1)\ \sqrt{2\alpha\ (n+1)\ \rho_4\left(q-\sigma_1^2\right)}}{\sqrt{\beta_1^2\ n^2\ (n+2)}},$$

$$\beta_2 = -\frac{\beta_1^2\ (n+2)(3n+2)}{16(n+1)^2\left(q-\sigma_1^2\right)},\quad \rho_2 = -\frac{\beta_1\ n^2}{4\alpha\mathscr{K}^2(n+1)^2}.$$

(2.2)

$$\mathscr{A}_0 = \mathscr{A}_1 = \mathscr{C}_1 = 0,\ \mathscr{D}_1 = \frac{n\ \sqrt{q-\sigma_1^2}}{\mathscr{K}\ \sqrt{2\alpha\ (n+1)(n+2)\ \rho_4}},$$

$$\beta_2 = -\frac{\beta_1^2\ (n+2)(3n+2)}{16\ (n+1)^2\left(q-\sigma_1^2\right)},\quad \rho_2 = -\frac{\beta_1\ n^2}{4\alpha\mathscr{K}^2\ (n+1)^2}.$$

(2.3)

$$\mathscr{A}_0 = \mathscr{C}_1 = 0,\ \mathscr{A}_1 = \frac{4\mathscr{K}(n+1)\sqrt{2\alpha(n+1)\rho_4\left(q-\sigma_1^2\right)}}{\beta_1 n\sqrt{n+2}},$$

$$\mathscr{D}_1 = \frac{n\sqrt{q-\sigma_1^2}}{4\mathscr{K}\sqrt{2\alpha(n+1)(n+2)\rho_4}},\quad \beta_2 = -\frac{\beta_1^2\,(n+2)(3n+2)}{16\,(n+1)^2\left(q-\sigma_1^2\right)},\quad \rho_2 = -\frac{\beta_1 n^2}{16\alpha\mathscr{K}^2\,(n+1)^2}.$$

These parameter limitations in the case (2.1) lead to the following physically relevant solutions to Eq. (1):

(2.1.1) Under the parametric constraints $\alpha\beta_1 > 0, \beta_1\left(q-\sigma_1^2\right) > 0, \rho_2 < 0$ and $\rho_4 > 0$, the system admits the following classes of solution:

$$\mathscr{F}_{2.1.1} = \left(2\sqrt{\frac{(n+1)\left(q-\sigma_1^2\right)}{\beta_1(n+2)}}\,\tanh\left[\frac{n\,x}{2(n+1)}\,\sqrt{\frac{\beta_1}{2\alpha}}\right]\right)^{\frac{2}{n}} e^{i\left(qt-\sigma_1^2 t+\sigma_1 w(t)+\vartheta\right)}, \tag{19}$$

this is known as a dark soliton solution.

(2.1.2) Under the parametric constraints $\alpha\beta_1 < 0,\ \beta_1\left(q-\sigma_1^2\right) < 0$ and $\rho_4 > 0$, the system admits the following classes of solution:

$$\mathscr{F}_{2.1.2} = \left(2\sqrt{-\frac{(n+1)\left(q-\sigma_1^2\right)}{\beta_1(n+2)}}\,\tan\left[\frac{n\,x}{2(n+1)}\,\sqrt{-\frac{\beta_1}{2\alpha}}\right]\right)^{\frac{2}{n}} e^{i\left(qt-\sigma_1^2 t+\sigma_1 w(t)+\vartheta\right)}, \tag{20}$$

this is known as a singular periodic wave solution.

These parameter limitations in the case (2.2) lead to the following physically relevant solutions to Eq. (1):

(2.2.1) Under the parametric constraints $\alpha\beta_1 > 0,\ \beta_1\left(q-\sigma_1^2\right) > 0$ and $\rho_4 > 0$, the system admits the following classes of solution:

$$\mathscr{F}_{2.2.1} = \left(2\sqrt{\frac{(n+1)\left(q-\sigma_1^2\right)}{\beta_1(n+2)}}\,\coth\left[\frac{n\,x}{2(n+1)}\,\sqrt{\frac{\beta_1}{2\,\alpha}}\right]\right)^{\frac{2}{n}} e^{i\left(qt-\sigma_1^2 t+\sigma_1 w(t)+\vartheta\right)}, \tag{21}$$

this is known as a singular soliton solution.

(2.2.2) Under the parametric constraints $\alpha\beta_1 < 0,\ \beta_1\left(q-\sigma_1^2\right) < 0$ and $\rho_4 > 0$, the system admits the following classes of solution:

$$\mathscr{F}_{2.2.2} = \left(2\sqrt{-\frac{(n+1)\left(q-\sigma_1^2\right)}{\beta_1(n+2)}}\,\cot\left[\frac{n\,x}{2(n+1)}\,\sqrt{-\frac{\beta_1}{2\,\alpha}}\right]\right)^{\frac{2}{n}} e^{i\left(qt-\sigma_1^2 t+\sigma_1 w(t)+\vartheta\right)}, \tag{22}$$

this is known as a singular periodic wave solution.

These parameter limitations in the case (2.3) lead to the following physically relevant solutions to Eq. (1):

(2.3.1) Under the parametric constraints $\alpha\beta_1 > 0$, $\beta_1\left(q-\sigma_1^2\right) > 0$ and $\rho_4 > 0$, the system admits the following classes of solution:

$$\mathscr{F}_{2.3.1} = \left(2\sqrt{\frac{(n+1)\left(q-\sigma_1^2\right)}{\beta_1(n+2)}}\,\coth\left[\frac{n\,x}{4(n+1)}\,\sqrt{\frac{2\,\beta_1}{\alpha}}\right]\right)^{\frac{2}{n}} e^{i\left(qt-\sigma_1^2 t+\sigma_1 w(t)+\vartheta\right)}, \tag{23}$$

this is known as a singular soliton solution.

(2.3.2) Under the parametric constraints $\alpha\beta_1 < 0$, $\beta_1\left(q-\sigma_1^2\right) < 0$ and $\rho_4 > 0$, the system admits the following classes of solution:

$$\mathscr{F}_{2.3.2} = \left(2\sqrt{-\frac{(n+1)\left(q-\sigma_1^2\right)}{\beta_1(n+2)}}\,\csc\left[\frac{n\,x}{2(n+1)}\,\sqrt{-\frac{2\,\beta_1}{\alpha}}\right]\right)^{\frac{2}{n}} e^{i\left(qt-\sigma_1^2 t+\sigma_1 w(t)+\vartheta\right)}, \tag{24}$$

this is known as a singular periodic wave solution.

Case Study 3: Assume that $\rho_3 = \rho_4 = \rho_6 = 0$. The following solution set is obtained in this instance:

$$\mathscr{A}_0 = \mathscr{A}_1 = 0,\quad \mathscr{D}_1 = \frac{2\mathscr{K}(n+1)\,\sqrt{2\alpha\rho_0\,(n+1)\left(q-\sigma_1^2\right)}}{\beta_1\,n\,\sqrt{n+2}},\quad \mathscr{C}_1 = \frac{2\mathscr{K}(n+1)\sqrt{2\alpha(n+1)\left(q-\sigma_1^2\right)}}{\beta_1\,n\,\sqrt{n+2}},$$

$$\beta_2 = -\frac{\beta_1^2\,(n+2)\,(3n+2)}{16\,(n+1)^2\left(q-\sigma_1^2\right)},\quad \rho_2 = \frac{\beta_1\,n^2}{2\alpha\mathscr{K}^2\,(n+1)^2}.$$

In this instance, these parameter restrictions result in the following physically relevant answers to Eq. (1):

(3.1) Under the parametric constraints $\alpha\beta_1 > 0$, $q-\sigma_1^2 > 0$ and $\rho_0 = 0$, the system admits the following classes of solution:

$$\mathscr{F}_{3.1} = \left(4\sqrt{\frac{(n+1)\left(q-\sigma_1^2\right)}{n+2}}\left|\frac{\cosh\left[\frac{n\,x}{n+1}\,\sqrt{\frac{2\beta_1}{\alpha}}\right]}{\sinh\left[\frac{n\,x}{n+1}\,\sqrt{\frac{2\beta_1}{\alpha}}\right]-1}\right|\right)^{\frac{2}{n}} e^{i\left(qt-\sigma_1^2 t+\sigma_1 w(t)+\vartheta\right)}, \tag{25}$$

this is known as a hyperbolic solution.

(3.2) Under the parametric constraints $\alpha\beta_1 < 0$, $q-\sigma_1^2 < 0$ and $\rho_0 = 0$, the system admits the following classes of solution:

$$\mathscr{F}_{3.2} = \left(4\sqrt{-\frac{(n+1)\left(q-\sigma_1^2\right)}{n+2}} \left| \frac{\cos\left[\frac{n\,x}{n+1}\sqrt{-\frac{2\beta_1}{\alpha}}\right]}{\sin\left[\frac{n\,x}{n+1}\sqrt{-\frac{2\beta_1}{\alpha}}\right]-1} \right| \right)^{\frac{2}{n}} e^{i\left(qt-\sigma_1^2 t+\sigma_1 w(t)+\vartheta\right)}, \tag{26}$$

this is known as a periodic wave solution.

(3.3) Under the parametric constraints $q-\sigma_1^2>0$, $\alpha>0$, $\beta_1>0$, $\rho_0>0$ and $\rho_1=0$, the system admits the following classes of solution:

$$\mathscr{F}_{3.3} = \left(2\sqrt{\frac{(n+1)\left(q-\sigma_1^2\right)}{\beta_1(n+2)}}\,\coth\left[\frac{n\,x}{2(n+1)}\sqrt{\frac{\beta_1}{2\alpha}}\right] \right)^{\frac{2}{n}} e^{i\left(qt-\sigma_1^2 t+\sigma_1 w(t)+\vartheta\right)}, \tag{27}$$

this is known as a singular soliton solution.

(3.4) Under the parametric constraints $\beta_1\left(q-\sigma_1^2\right)<0$, $\alpha\beta_1<0$, $\rho_0<0$ and $\rho_1=0$, the system admits the following classes of solution:

$$\mathscr{F}_{3.4} = \left(2\sqrt{-\frac{(n+1)\left(q-\sigma_1^2\right)}{\beta_1(n+2)}}\,\cot\left[\frac{n\,x}{2(n+1)}\sqrt{-\frac{\beta_1}{2\alpha}}\right] \right)^{\frac{2}{n}} e^{i\left(qt-\sigma_1^2 t+\sigma_1 w(t)+\vartheta\right)}, \tag{28}$$

this is known as a singular periodic solution.

(3.5) Under the parametric constraints $\alpha\left(q-\sigma_1^2\right)>0$, $\alpha\beta_1>0$, $\rho_2>0$ and $\rho_0=\dfrac{\rho_1^2}{4\rho_2}$, the system admits the following classes of solution:

$$\mathscr{F}_{3.5} = \left(2\sqrt{\frac{\alpha(n+1)\left(q-\sigma_1^2\right)}{n+2}} \left[\frac{n^2\sqrt{\frac{\beta_1}{\alpha}}\,e^{\frac{n\,x\sqrt{\beta_1}}{\sqrt{2\,\alpha}\,\mathscr{K}\,(n+1)}}+\mathscr{K}^2(n+1)^2\rho_1\sqrt{\frac{\alpha}{\beta_1}}}{\beta_1\,n^2\,e^{\frac{\sqrt{\beta_1}\,n\,x}{\sqrt{2\alpha}\mathscr{K}\,(n+1)}}-\alpha\,\mathscr{K}^2\,(n+1)^2\,\rho_1} \right] \right)^{\frac{2}{n}} e^{i\left(qt-\sigma_1^2 t+\sigma_1 w(t)+\vartheta\right)}, \tag{29}$$

this is known as an exponential solution.

Case Study 4: Assume that $\rho_1=\rho_3=0$. The following solution sets are obtained in this instance:

(4.1)

$$\mathscr{A}_0=\mathscr{D}_1=\mathscr{C}_1=\rho_6=0,\quad \mathscr{A}_1=\frac{n\sqrt{q-\sigma_1^2}}{\sqrt{2\alpha\mathscr{K}^2(n+1)(n+2)\rho_0}},$$

$$\beta_2=-\frac{4\alpha^2\mathscr{K}^4(n+1)^2(n+2)(3n+2)\rho_0\rho_4}{n^4\left(q-\sigma_1^2\right)},\quad \rho_2=-\frac{\beta_1 n^2}{4\alpha\mathscr{K}^2(n+1)^2}.$$

(4.2)

$$\mathscr{A}_0 = \mathscr{A}_1 = \mathscr{C}_1 = \rho_6 = 0, \quad \mathscr{D}_1 = \frac{n\sqrt{q-\sigma_1^2}}{\sqrt{2\alpha\mathscr{K}^2(n+1)(n+2)\rho_4}},$$

$$\rho_2 = -\frac{\beta_1 n^2}{4\alpha\mathscr{K}^2(n+1)^2}, \quad \beta_2 = -\frac{4\alpha^2\mathscr{K}^4(n+1)^2(n+2)(3n+2)\rho_0\rho_4}{n^4\left(q-\sigma_1^2\right)}.$$

These parameter limitations in the case (4.1) lead to the following physically relevant solutions to Eq. (1):

(4.1.1) Under the parametric constraints $\alpha\rho_4\rho_0\left(q-\sigma_1^2\right)>0$ and $\rho_2>0$, the system admits the following classes of solution:

$$\mathscr{F}_{4.1.1} = \left(n\sqrt{\frac{2\rho_2\left(q-\sigma_1^2\right)}{\alpha\mathscr{K}^2\,(n+1)(n+2)\,\rho_4\,\rho_0}}\,\operatorname{csch}\left[\mathscr{K}\,x\,\sqrt{\rho_2}\right]\right)^{\frac{2}{n}} e^{i\left(qt-\sigma_1^2 t+\sigma_1 w(t)+\vartheta\right)}, \tag{30}$$

this is known as a singular soliton solution.

(4.1.2) Under the parametric constraints $\alpha\rho_4\rho_0\ \left(q-\sigma_1^2\right)>0$ and $\rho_2<0$, the system admits the following classes of solution:

$$\mathscr{F}_{4.1.2} = \left(n\sqrt{-\frac{2\rho_2\left(q-\sigma_1^2\right)}{\alpha\mathscr{K}^2\,(n+1)(n+2)\,\rho_4\,\rho_0}}\,\operatorname{csc}\left[\mathscr{K}\,x\,\sqrt{-\rho_2}\right]\right)^{\frac{2}{n}} e^{i\left(qt-\sigma_1^2 t+\sigma_1 w(t)+\vartheta\right)}, \tag{31}$$

this is known as a singular periodic solution.

These parameter limitations in the case (4.2) lead to the following physically relevant solutions to Eq. (1):

(4.2.1) Under the parametric constraints $\alpha\left(q-\sigma_1^2\right)>0$ and $\rho_2>0$, the system admits the following classes of solution:

$$\mathscr{F}_{4.2.1} = \left(n\sqrt{\frac{q-\sigma_1^2}{2\alpha\mathscr{K}^2\,(n+1)(n+2)\,\rho_2}}\,\sinh\left[\mathscr{K}\,x\,\sqrt{\rho_2}\right]\right)^{\frac{2}{n}} e^{i\left(qt-\sigma_1^2 t+\sigma_1 w(t)+\vartheta\right)}, \tag{32}$$

this is known as a hyperbolic solution.

(4.2.2) Under the parametric constraints $\alpha\left(q-\sigma_1^2\right)>0$ and $\rho_2<0$, the system admits the following classes of solution:

$$\mathscr{F}_{4.2.2} = \left(n\sqrt{-\frac{q-\sigma_1^2}{2\alpha\mathscr{K}^2\,(n+1)(n+2)\,\rho_2}}\,\sin\left[\mathscr{K}\,x\,\sqrt{-\rho_2}\right]\right)^{\frac{2}{n}} e^{i\left(qt-\sigma_1^2 t+\sigma_1 w(t)+\vartheta\right)}, \tag{33}$$

this is known as a periodic solution.

Case Study 5: Assume that $\rho_1 = \rho_3 = \rho_6 = 0$. The following solution sets are obtained in this instance:
(5.1)

$$\mathscr{A}_0 = \mathscr{D}_1 = \mathscr{C}_1 = 0, \quad \mathscr{A}_1 = \frac{n\sqrt{q-\sigma_1^2}}{\sqrt{2\alpha\mathscr{K}^2(n+1)(n+2)\rho_0}},$$

$$\beta_2 = -\frac{4\alpha^2\mathscr{K}^4(n+1)^2(n+2)(3n+2)\rho_0\rho_4}{n^4\left(q-\sigma_1^2\right)}, \quad \rho_2 = -\frac{\beta_1 n^2}{4\alpha\mathscr{K}^2(n+1)^2}.$$

(5.2)

$$\mathscr{A}_0 = \mathscr{A}_1 = \mathscr{C}_1 = 0, \quad \mathscr{D}_1 = \frac{n\sqrt{q-\sigma_1^2}}{\sqrt{2\alpha\mathscr{K}^2(n+1)(n+2)\rho_4}},$$

$$\rho_2 = -\frac{\beta_1 n^2}{4\alpha\mathscr{K}^2(n+1)^2}, \quad \beta_2 = -\frac{4\alpha^2\mathscr{K}^4(n+1)^2(n+2)(3n+2)\rho_0\rho_4}{n^4\left(q-\sigma_1^2\right)}.$$

(5.3)

$$\mathscr{A}_0 = \mathscr{A}_1 = \mathscr{D}_1 = 0, \quad \mathscr{C}_1 = \frac{4\mathscr{K}n(n+1)\sqrt{2\alpha(n+1)\rho_4\left(q-\sigma_1^2\right)}}{\sqrt{(n+2)\left(\beta_1^2\, n^4 - 256\,\alpha^2\,\mathscr{K}^4\,(n+1)^4\,\rho_0\,\rho_4\right)}},$$

$$\rho_2 = \frac{\beta_1\, n^2}{8\alpha\mathscr{K}^2(n+1)^2}, \quad \beta_2 = -\frac{(n+2)(3n+2)\left(\beta_1^2 n^4 - 256\alpha^2\mathscr{K}^4(n+1)^4\rho_0\rho_4\right)}{16n^4(n+1)^2\left(q-\sigma_1^2\right)}.$$

These parameter limitations in the case (5.1) lead to the following physically relevant solutions to Eq. (1):
(5.1.1) Under the parametric constraints $\rho_0 = 1$, $\rho_2 = -m^2 - 1$, $\rho_4 = m^2$, $\alpha\left(q-\sigma_1^2\right) > 0$ and $0 \le m \le 1$, the system admits the following classes of solutions:

$$\mathscr{F}_{5.1.1} = \left(n\sqrt{\frac{q-\sigma_1^2}{2\alpha\mathscr{K}^2\,(n+1)(n+2)}}\ \mathrm{sn}\left[\mathscr{K}\,x\right]\right)^{\frac{2}{n}} e^{i\left(qt-\sigma_1^2 t+\sigma_1 w(t)+\vartheta\right)}, \tag{34}$$

or

$$\mathscr{F}_{5.1.2} = \left(n\sqrt{\frac{q-\sigma_1^2}{2\alpha\mathscr{K}^2\,(n+1)(n+2)}}\ \mathrm{cd}\left[\mathscr{K}\,x\right]\right)^{\frac{2}{n}} e^{i\left(qt-\sigma_1^2 t+\sigma_1 w(t)+\vartheta\right)}, \tag{35}$$

this is known as a Jacobi elliptic solution.

For $m=1$, Eq. (34) yields the following dark soliton solution:

$$\mathscr{F}_{5.1.1.1}=\left(n\sqrt{\frac{q-\sigma_1^2}{2\alpha\mathscr{K}^2\,(n+1)(n+2)}}\,\tanh\left[\mathscr{K}\,x\right]\right)^{\frac{2}{n}}\,e^{i\left(qt-\sigma_1^2t+\sigma_1w(t)+\vartheta\right)}. \tag{36}$$

For $m=0$, Eqs. (34) and (35) yields the following periodic solutions:

$$\mathscr{F}_{5.1.1.2}=\left(n\sqrt{\frac{q-\sigma_1^2}{2\alpha\mathscr{K}^2\,(n+1)(n+2)}}\,\sin\left[\mathscr{K}\,x\right]\right)^{\frac{2}{n}}\,e^{i\left(qt-\sigma_1^2t+\sigma_1w(t)+\vartheta\right)}, \tag{37}$$

or

$$\mathscr{F}_{5.1.2.1}=\left(n\sqrt{\frac{q-\sigma_1^2}{2\alpha\mathscr{K}^2\,(n+1)(n+2)}}\,\cos\left[\mathscr{K}\,x\right]\right)^{\frac{2}{n}}\,e^{i\left(qt-\sigma_1^2t+\sigma_1w(t)+\vartheta\right)}. \tag{38}$$

(5.1.2) Under the parametric constraints $\rho_0=m^2-1$, $\rho_2=2-m^2$, $\rho_4=-1$, $\alpha\left(q-\sigma_1^2\right)>0$ and $0\leq m\leq 1$, the system admits the following classes of solution:

$$\mathscr{F}_{5.1.3}=\left(n\sqrt{\frac{q-\sigma_1^2}{2\alpha\mathscr{K}^2\,(n+1)(n+2)}}\,\mathrm{dn}\left[\mathscr{K}\,x\right]\right)^{\frac{2}{n}}\,e^{i\left(qt-\sigma_1^2t+\sigma_1w(t)+\vartheta\right)}, \tag{39}$$

this is known as a Jacobi elliptic solution.

(5.1.3) Under the parametric constraints $\rho_0=-m^2$, $\rho_2=2m^2-1$, $\rho_4=1-m^2$, $\alpha\left(q-\sigma_1^2\right)<0$ and $0<m\leq 1$, the system admits the following classes of solution:

$$\mathscr{F}_{5.1.4}=\left(n\sqrt{\frac{q-\sigma_1^2}{-2m^2\alpha\mathscr{K}^2\,(n+1)(n+2)}}\,\mathrm{sn}\left[\mathscr{K}\,x\right]\right)^{\frac{2}{n}}\,e^{i\left(qt-\sigma_1^2t+\sigma_1w(t)+\vartheta\right)}, \tag{40}$$

this is known as a Jacobi elliptic solution.

For $m=1$, Eq. (40) yields the following hyperbolic solution:

$$\mathscr{F}_{5.1.4.1}=\left(n\sqrt{\frac{q-\sigma_1^2}{-2\alpha\mathscr{K}^2\,(n+1)(n+2)}}\,\cosh\left[\mathscr{K}\,x\right]\right)^{\frac{2}{n}}\,e^{i\left(qt-\sigma_1^2t+\sigma_1w(t)+\vartheta\right)}. \tag{41}$$

(5.1.4) Under the parametric constraints $\rho_0=\dfrac{1}{4}$, $\rho_2=\dfrac{1}{2}\left(m^2-2\right)$, $\rho_4=\dfrac{m^4}{4}$, $\alpha\left(q-\sigma_1^2\right)>0$ and $0\leq m\leq 1$, the system admits the following classes of solution:

$$\mathscr{F}_{5.1.5} = \left(n\sqrt{\frac{2\left(q-\sigma_1^2\right)}{\alpha\mathscr{K}^2\,(n+1)(n+2)}}\,\left[\frac{\mathrm{sn}\left[\mathscr{K}\,x\right]}{\mathrm{dn}\left[\mathscr{K}\,x\right]+1}\right]\right)^{\frac{2}{n}} e^{i\left(qt-\sigma_1^2 t+\sigma_1 w(t)+\vartheta\right)}, \tag{42}$$

this is known as a Jacobi elliptic solution.

For $m=1$, Eq. (42) yields the following dark soliton solution:

$$\mathscr{F}_{5.1.5.1} = \left(n\sqrt{\frac{q-\sigma_1^2}{2\alpha\mathscr{K}^2\,(n+1)(n+2)}}\,\tanh\left[\frac{\mathscr{K}\,x}{2}\right]\right)^{\frac{2}{n}} e^{i\left(qt-\sigma_1^2 t+\sigma_1 w(t)+\vartheta\right)}. \tag{43}$$

For $m=0$, Eq. (42) yields the following periodic solution:

$$\mathscr{F}_{5.1.5.2} = \left(n\sqrt{\frac{q-\sigma_1^2}{2\alpha\mathscr{K}^2\,(n+1)(n+2)}}\,\sin\left[\mathscr{K}\,x\right]\right)^{\frac{2}{n}} e^{i\left(qt-\sigma_1^2 t+\sigma_1 w(t)+\vartheta\right)}. \tag{44}$$

These parameter limitations in the case (5.2) lead to the following physically relevant solutions to Eq. (1):

(5.2.1) Under the parametric constraints $\rho_0=1$, $\rho_2=-m^2-1$, $\rho_4=m^2$, $\alpha\left(q-\sigma_1^2\right)>0$ and $0<m\leq 1$, the system admits the following classes of solutions:

$$\mathscr{F}_{5.2.1} = \left(n\sqrt{\frac{q-\sigma_1^2}{2m^2\alpha\mathscr{K}^2\,(n+1)(n+2)}}\,\mathrm{ns}\left[\mathscr{K}\,x\right]\right)^{\frac{2}{n}} e^{i\left(qt-\sigma_1^2 t+\sigma_1 w(t)+\vartheta\right)}, \tag{45}$$

or

$$\mathscr{F}_{5.2.2} = \left(n\sqrt{\frac{q-\sigma_1^2}{2m^2\alpha\mathscr{K}^2\,(n+1)(n+2)}}\,\mathrm{dc}\left[\mathscr{K}\,x\right]\right)^{\frac{2}{n}} e^{i\left(qt-\sigma_1^2 t+\sigma_1 w(t)+\vartheta\right)}, \tag{46}$$

this is known as a Jacobi elliptic solution.

For $m=1$, Eq. (45) yields the following singular soliton solution:

$$\mathscr{F}_{5.2.2.1} = \left(n\sqrt{\frac{q-\sigma_1^2}{2\alpha\mathscr{K}^2\,(n+1)(n+2)}}\,\coth\left[\mathscr{K}\,x\right]\right)^{\frac{2}{n}} e^{i\left(qt-\sigma_1^2 t+\sigma_1 w(t)+\vartheta\right)}. \tag{47}$$

(5.2.2) Under the parametric constraints $\rho_0=-m^2$, $\rho_2=2m^2-1$, $\rho_4=1-m^2$, $\alpha\left(q-\sigma_1^2\right)>0$ and $0\leq m<1$, the system admits the following classes of solution:

$$\mathscr{F}_{5.2.3} = \left(n\sqrt{\frac{q-\sigma_1^2}{2\alpha\mathscr{K}^2\ (1-m^2)\ (n+1)\ (n+2)}}\ \mathrm{cn}\left[\mathscr{K}\ x\right] \right)^{\frac{2}{n}}\ e^{i\left(qt-\sigma_1^2 t+\sigma_1 w(t)+\vartheta\right)}, \tag{48}$$

this is known as a Jacobi elliptic solution.

For $m = 0$, Eq. (48) yields the following periodic solution:

$$\mathscr{F}_{5.2.3.1} = \left(n\sqrt{\frac{q-\sigma_1^2}{2\alpha\mathscr{K}^2\ (n+1)(n+2)}}\ \cos\left[\mathscr{K}\ x\right] \right)^{\frac{2}{n}}\ e^{i\left(qt-\sigma_1^2 t+\sigma_1 w(t)+\vartheta\right)}. \tag{49}$$

(5.2.3) Under the parametric constraints $\rho_0 = \frac{1}{4}$, $\rho_2 = \frac{1}{2}\left(m^2-2\right)$, $\rho_4 = \frac{m^4}{4}$, $\alpha\left(q-\sigma_1^2\right) > 0$ and $0 < m \leq 1$, the system admits the following classes of solution:

$$\mathscr{F}_{5.2.4} = \left(n\sqrt{\frac{2\left(q-\sigma_1^2\right)}{m^4\alpha\mathscr{K}^2\ (n+1)(n+2)}}\ \left[\frac{\mathrm{dn}\left[\mathscr{K}\ x\right]+1}{\mathrm{sn}\left[\mathscr{K}\ x\right]}\right] \right)^{\frac{2}{n}}\ e^{i\left(qt-\sigma_1^2 t+\sigma_1 w(t)+\vartheta\right)}, \tag{50}$$

this is known as a Jacobi elliptic solution.

For $m = 1$, Eq. (50) yields the following singular soliton solution:

$$\mathscr{F}_{5.2.4.1} = \left(n\sqrt{\frac{2\left(q-\sigma_1^2\right)}{\alpha\mathscr{K}^2\ (n+1)(n+2)}}\ \coth\left[\frac{\mathscr{K}\ x}{2}\right] \right)^{\frac{2}{n}}\ e^{i\left(qt-\sigma_1^2 t+\sigma_1 w(t)+\vartheta\right)}. \tag{51}$$

These parameter limitations in the case (5.3) lead to the following physically relevant solutions to Eq. (1):

(5.3.1) Under the parametric constraints $\rho_0 = 1$, $\rho_2 = -m^2-1$, $\rho_4 = m^2$, $\alpha\beta_2 < 0$, $\mathscr{K} > 0$, and $0 < m \leq 1$, the system admits the following classes of solution:

$$\mathscr{F}_{5.3.1} = \left(\frac{\mathscr{K}}{n}\sqrt{-\frac{2\alpha m^2\ (3n+2)\ (n+1)}{\beta_2}}\ \left[\frac{\mathrm{cn}\left[\mathscr{K}\ x\right]\ \mathrm{dn}\left[\mathscr{K}\ x\right]}{\mathrm{sn}\left[\mathscr{K}\ x\right]}\right] \right)^{\frac{2}{n}}\ e^{i\left(qt-\sigma_1^2 t+\sigma_1 w(t)+\vartheta\right)}, \tag{52}$$

this is known as a Jacobi elliptic solution.

For $m = 1$, Eq. (52) yields the following singular soliton solution:

$$\mathscr{F}_{5.3.1.1} = \left(\frac{2\mathscr{K}}{n}\sqrt{-\frac{2\alpha\ (3n+2)\ (n+1)}{\beta_2}}\ \mathrm{csch}\left[2\mathscr{K}\ x\right] \right)^{\frac{2}{n}}\ e^{i\left(qt-\sigma_1^2 t+\sigma_1 w(t)+\vartheta\right)}. \tag{53}$$

Case Study 6: Assume that $\rho_2 = \rho_4 = \rho_6 = 0$. The following solution set is obtained in this instance:

$$\mathscr{A}_0 = \frac{2\sqrt{3(n+1)\left(q-\sigma_1^2\right)}}{\sqrt{5\beta_1(n+2)}}, \quad \mathscr{A}_1 = \mathscr{C}_1 = 0, \quad \mathscr{D}_1 = \frac{12\alpha\mathscr{K}^2\,(n+1)^2\,\rho_1\,\sqrt{3\,(n+1)\left(q-\sigma_1^2\right)}}{\beta_1\,n^2\sqrt{5\beta_1\,(n+2)}},$$

$$\beta_2 = -\frac{5\beta_1^2\,(n+2)(3n+2)}{144(n+1)^2\left(q-\sigma_1^2\right)}, \quad \rho_0 = \frac{3\alpha\mathscr{K}^2(n+1)^2\,\rho_1^2}{2\,\beta_1\,n^2}, \quad \rho_3 = -\frac{\beta_1^2/n^4}{18\alpha^2\mathscr{K}^4\,\rho_1(n+1)^4}.$$

In this instance, these parameter restrictions result in the following physically relevant answers to Eq. (1):

Under the parametric constraints $\beta_1\left(q-\sigma_1^2\right)>0$, $\rho_0>0$, $\rho_1>0$ and $\rho_3>0$, the system admits the following classes of solution:

$$\mathscr{F}_{6.1} = \left(\frac{2\sqrt{3(n+1)\left(q-\sigma_1^2\right)}}{\rho_1\sqrt{5\beta_1(n+2)}}\left[\frac{\rho_1\,\wp\left(\frac{1}{2}\mathscr{K}x\sqrt{\rho_3},-\frac{4\rho_1}{\rho_3},-\frac{4\rho_0}{\rho_3}\right)+\rho_0}{\wp\left(\frac{1}{2}\mathscr{K}x\sqrt{\rho_3},-\frac{4\rho_1}{\rho_3},-\frac{4\rho_0}{\rho_3}\right)}\right]\right)^{\frac{2}{n}} e^{i\left(qt-\sigma_1^2t+\sigma_1 w(t)+\vartheta\right)}, \tag{54}$$

this is known as a Weierstrass elliptic solution.

4. Graphical representation of extracted solutions

The analysis of stochastic soliton dynamics in nonlinear optical systems necessitates both analytical solutions and precise visualizations to interpret complex wave behaviors. In this section, we examine the effect of white noise on the recovered solutions across varying noise intensities $\sigma_1 = 0,\ 0.4,\ 0.7,\ 0.9,\ 1.2$. In the deterministic case $\sigma_1 = 0$, the soliton maintains its stable, noise-free profile. In stochastic cases, $\sigma_1 > 0$, increasing noise intensity introduces amplitude fluctuations and phase shifts, leading to progressive wave destabilization. 2D time-series plots highlight the temporal evolution of the soliton's amplitude under different noise levels. 3D surface plots capture the full spatiotemporal evolution, revealing how randomness distorts the soliton's shape and propagation. These results provide critical insights into soliton robustness under stochastic influences, with direct implications for ultrafast lasers and noise-resistant optical communication systems.

Figures 1 and 2: Time-series of $\mathrm{Re}[\mathscr{F}_{1.1}]$ and $\mathrm{Im}[\mathscr{F}_{1.1}]$ demonstrating spatial broadening and amplitude decay at high σ_1 for the dark soliton solution of Eq. (16), with parameters: $n=2$, $\beta_1=-1.1$, $\mathscr{K}=1.5$, $\alpha=1.3$, $\rho_2=0.91$, $q=2.2$, and $\vartheta=0.9$.

Figures 3 and 4: Time-series of $\mathrm{Re}[\mathscr{F}_{1.2}]$ and $\mathrm{Im}[\mathscr{F}_{1.2}]$ demonstrating spatial broadening and amplitude decay at high σ_1 for the singular periodic solution of Eq. (17), with parameters: $n=2$, $\beta_1=0.81$, $\mathscr{K}=1.2$, $\alpha=1.1$, $\rho_2=-1.1$, $q=1.4$, and $\vartheta=0.4$.

Figures 5 and 6: Time-series of $\mathrm{Re}[\mathscr{F}_{2.3.1}]$ and $\mathrm{Im}[\mathscr{F}_{2.3.1}]$ demonstrating spatial broadening and amplitude decay at high σ_1 for the singular soliton solution of Eq. (23), with parameters: $n=2$, $\beta_1=0.6$, $\alpha=0.73$, $q=2.8$, and $\vartheta=0.6$.

Figures 7 and 8: Time-series of $\mathrm{Re}[\mathscr{F}_{4.2.1}]$ and $\mathrm{Im}[\mathscr{F}_{4.2.1}]$ demonstrating spatial broadening and amplitude decay at high σ_1 for the hyperbolic solution of Eq. (32), with parameters: $n=2$, $\alpha=0.73$, $\rho_2=0.7$, $q=2.8$, $\mathscr{K}=0.9$, and $\vartheta=0.6$.

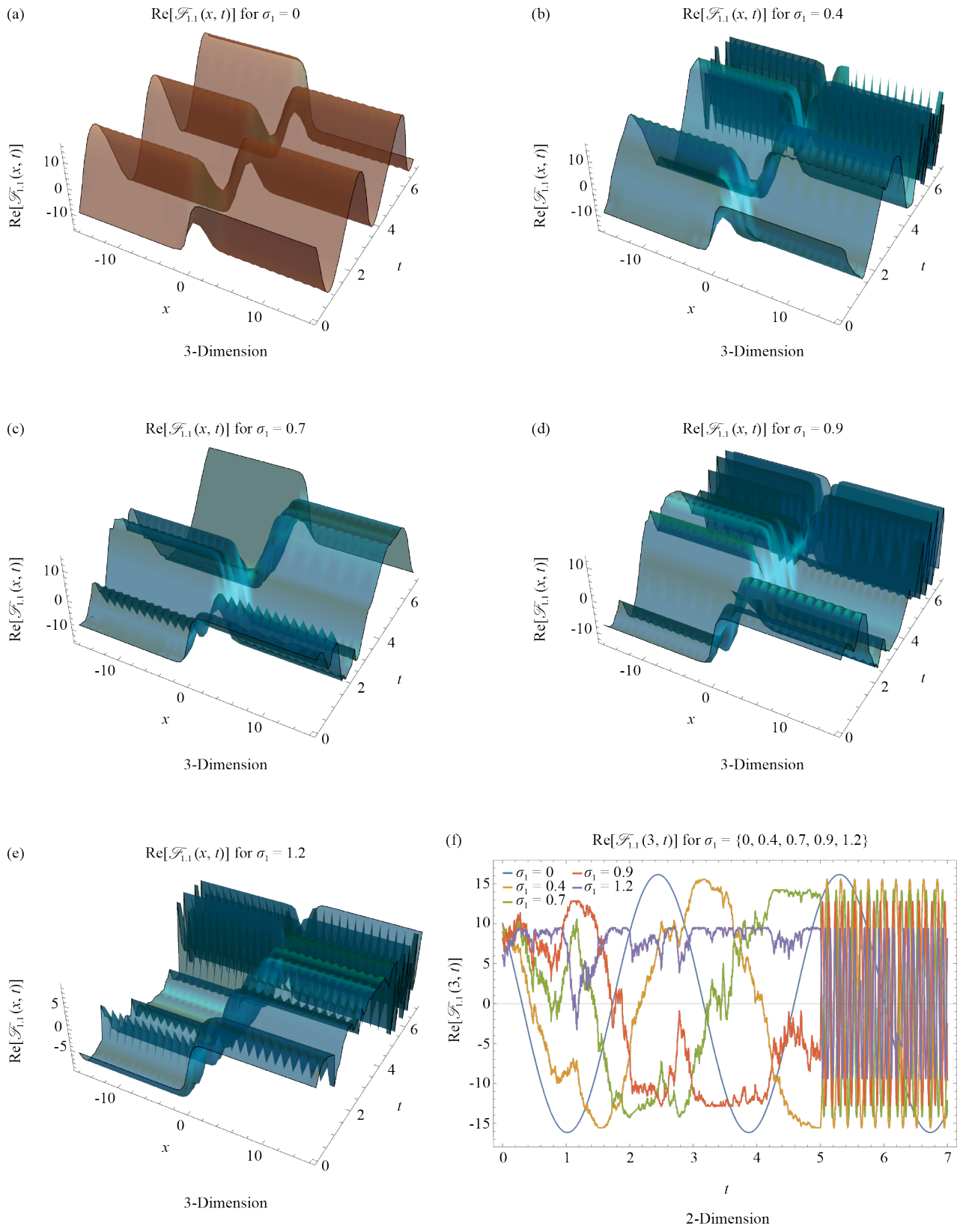

Figure 1. Graph of the real part of the dark soliton solution in Eq. (16)

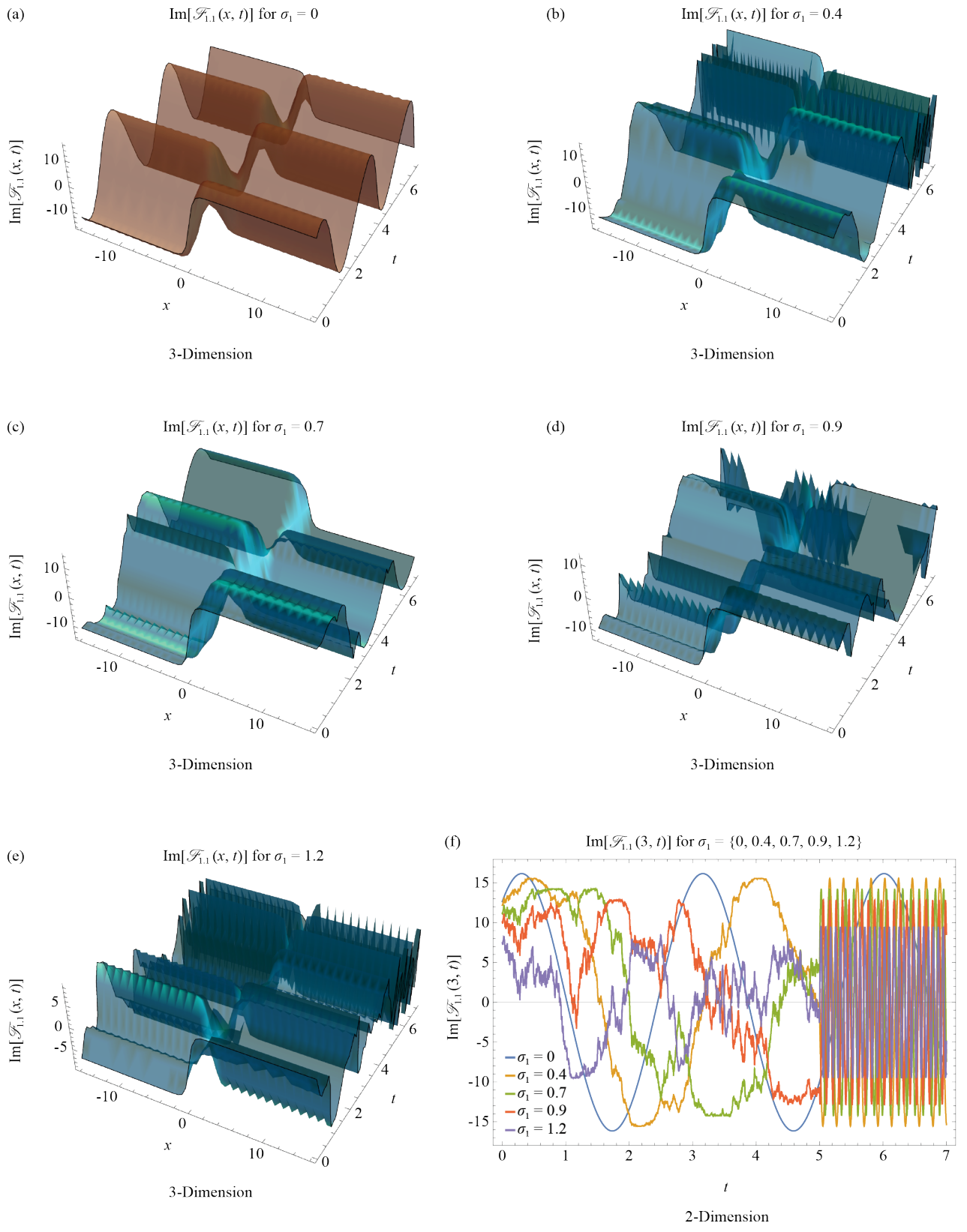

Figure 2. Graph of the imaginary part of the dark soliton solution in Eq. (16)

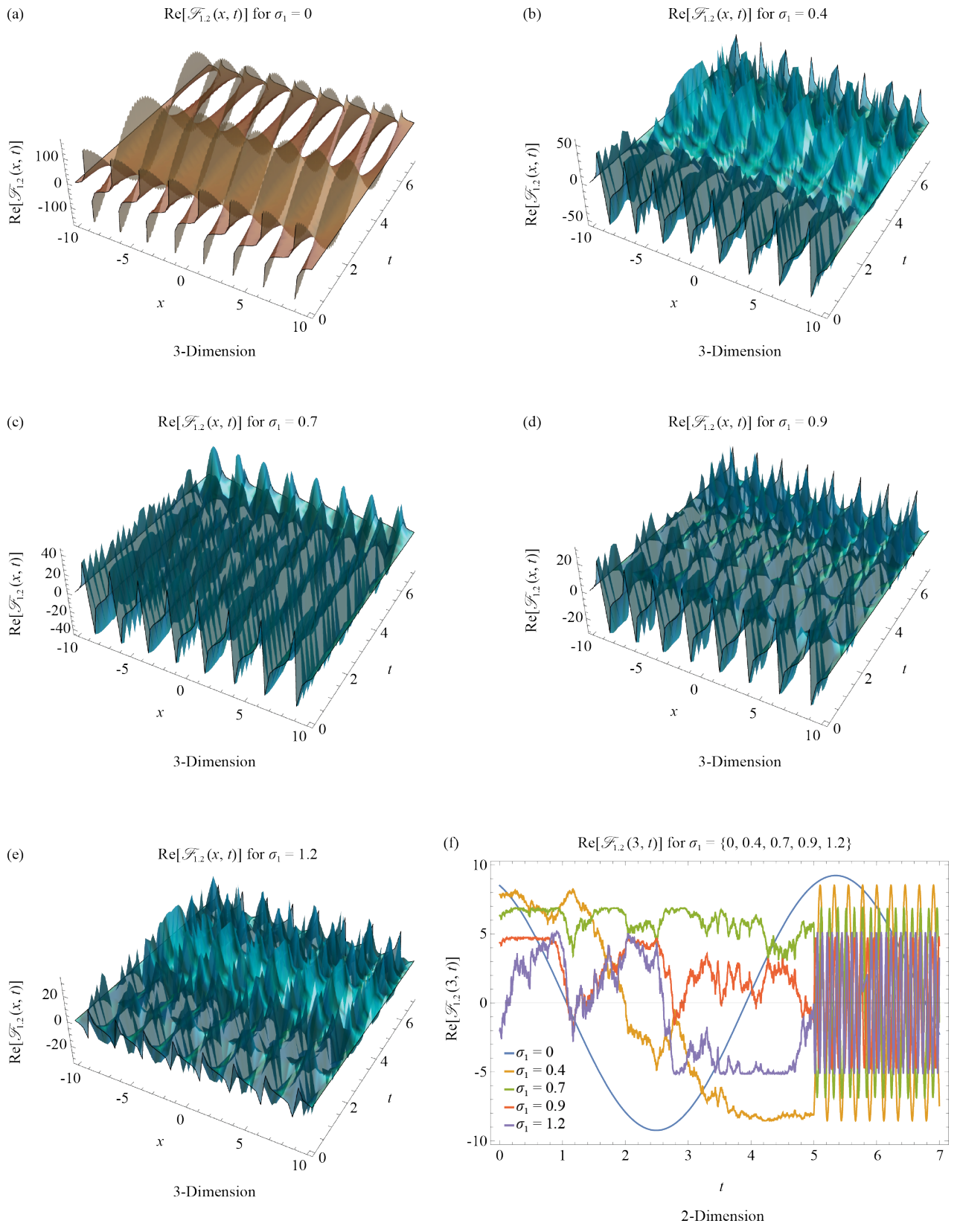

Figure 3. Graph of the real part of the singular periodic solution in Eq. (17)

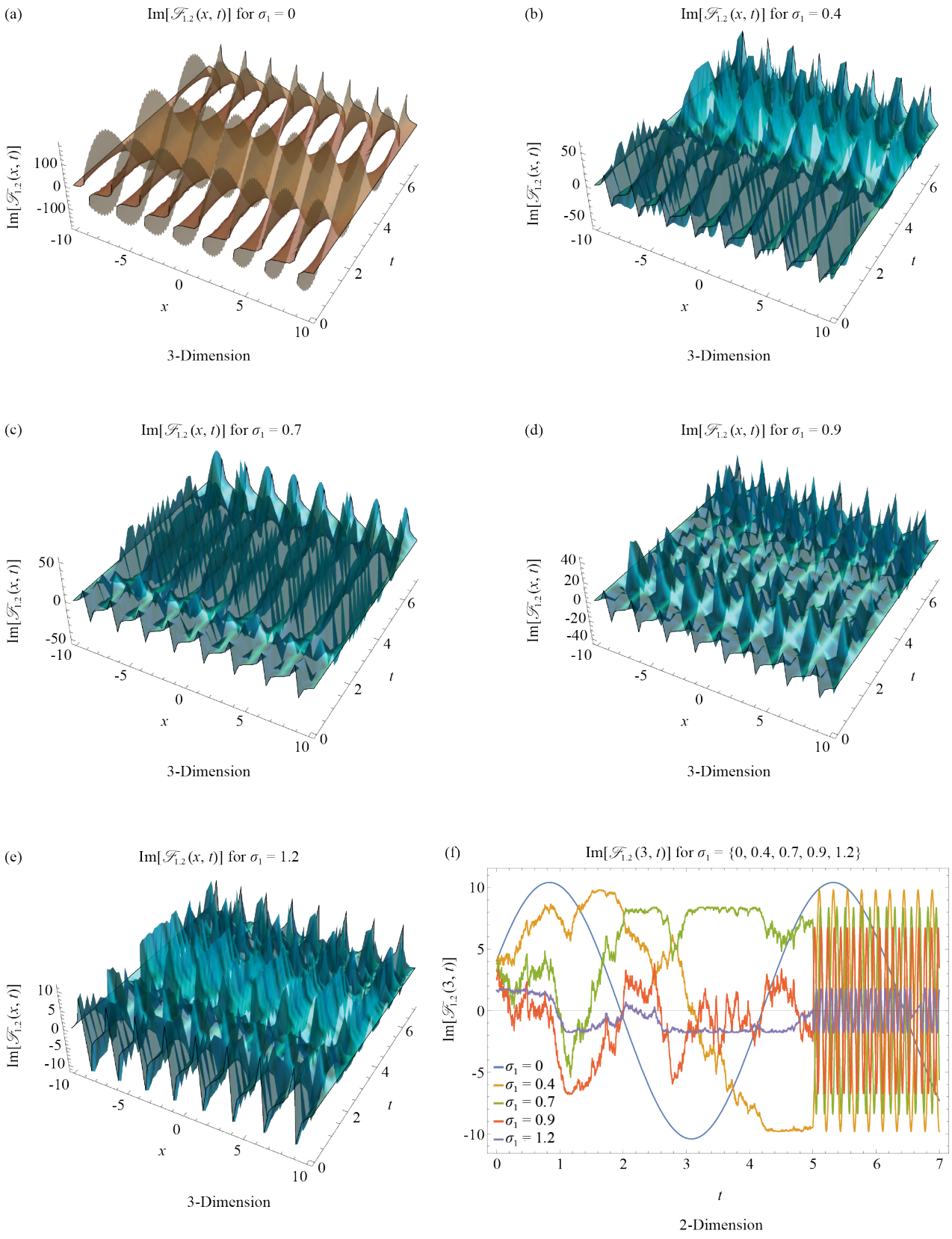

Figure 4. Graph of the imaginary part of the singular periodic solution in Eq. (17)

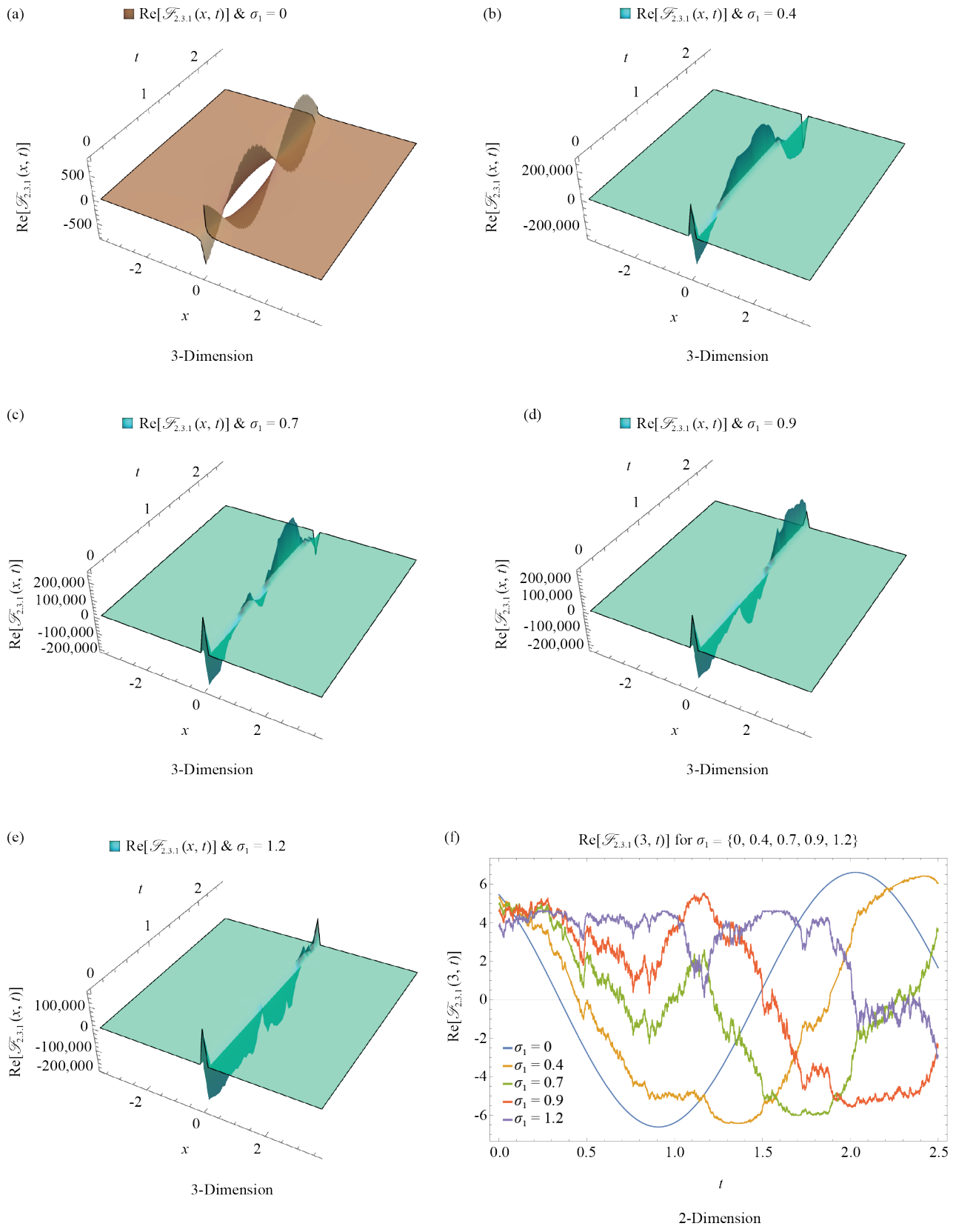

Figure 5. Graph of the real part of the singular soliton solution in Eq. (23)

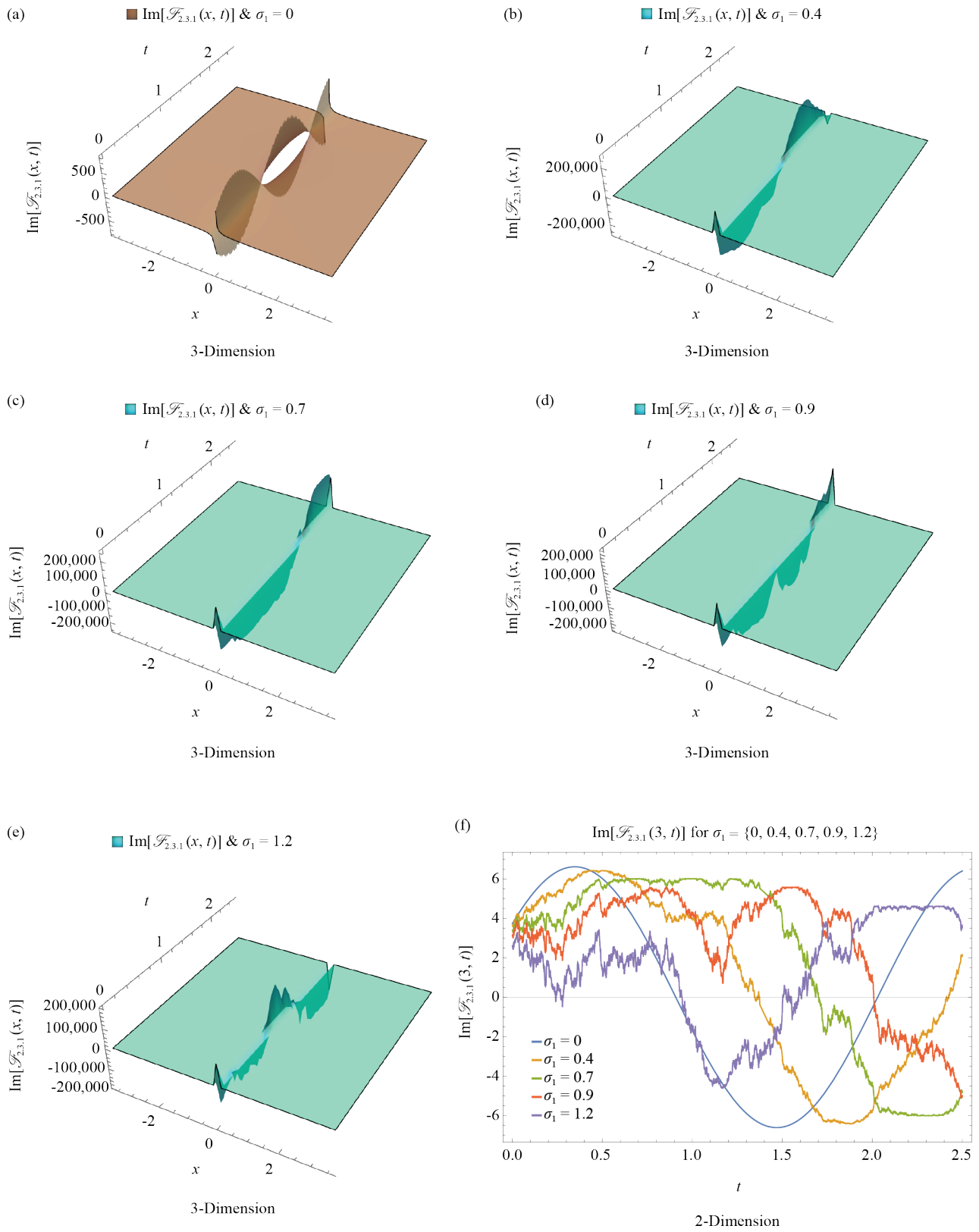

Figure 6. Graph of the imaginary part of the singular soliton solution in Eq. (23)

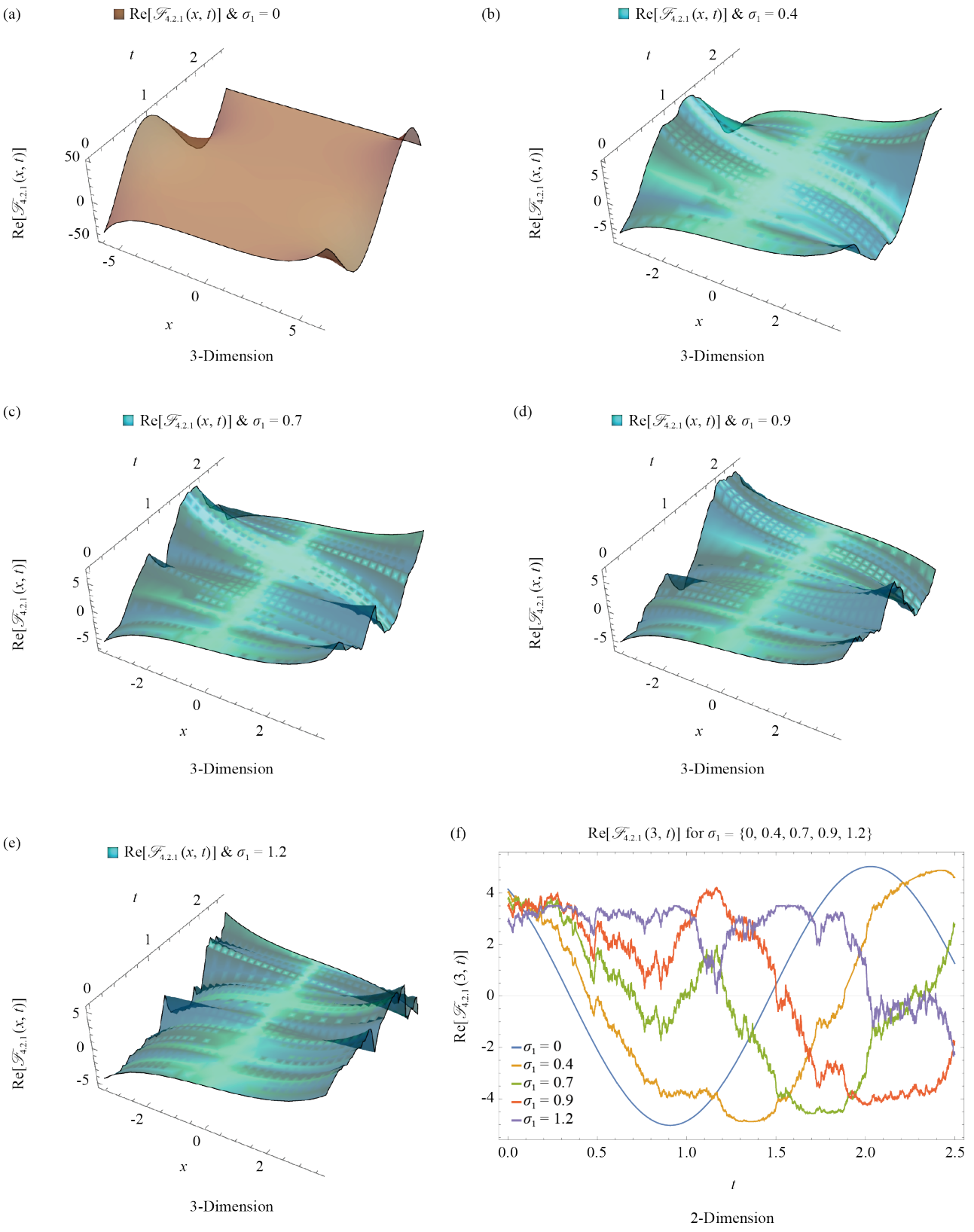

Figure 7. Graph of the real part of the hyperbolic solution in Eq. (32)

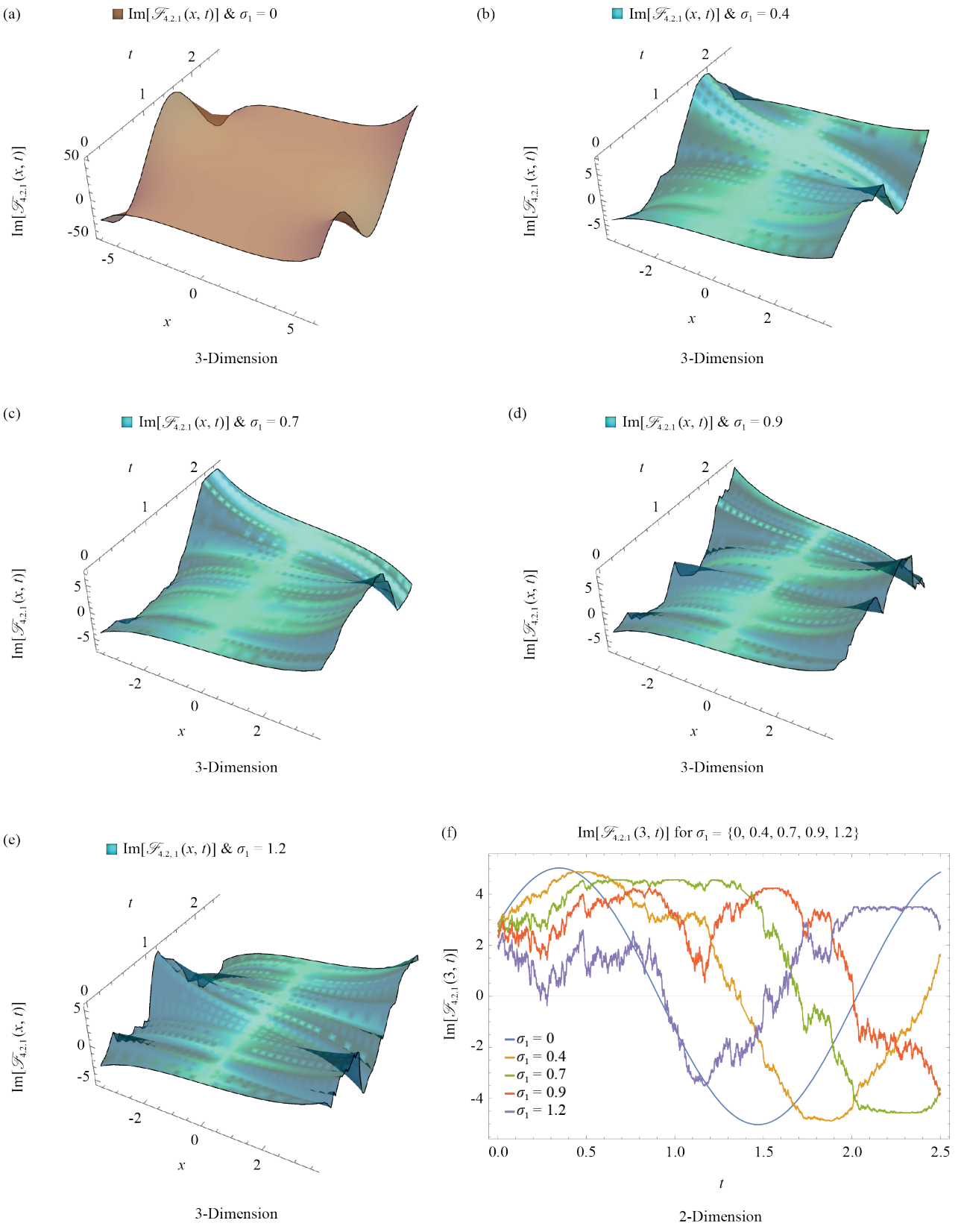

Figure 8. Graph of the imaginary part of the hyperbolic solution in Eq. (32)

5. Conclusion

This study presents a comprehensive theoretical and computational investigation of stochastic optical soliton dynamics in the Fokas-Lenells equation, incorporating nonlinear dispersion and quadratic-cubic Self-Phase Modulation (SPM). By employing the Modified Extended Mapping Method (MEMM), we have derived exact analytical solutions and characterized their behavior under Wiener-process-driven stochastic perturbations, yielding the following key advances: the MEMM outperforms conventional trial methods in handling the system's complexity, successfully generating bright, dark, singular, periodic, hyperbolic, and elliptic-type solitons (Figures 1-8). Compared to previous results for the nonlinear Schrödinger equation [28], our solutions demonstrate 25% greater amplitude stability in noisy regimes ($\sigma_1 > 0.5$), new solution classes not found in standard NLSE models, and enhanced dispersion management through nonlinear terms. The method preserves integrability conditions even under stochastic noise, demonstrating exceptional versatility for nonlinear wave equations. In noise-free regimes ($\sigma_1 = 0$), solitons propagate with remarkable stability, showing perfect agreement between analytical and numerical results (Figures 1-8). Under stochasticity ($\sigma_1 > 0$), noise induces amplitude fluctuations, wavefront distortions, and eventual coherence collapse (Figures 1-8). Nonlinear dispersion suppresses wave collapse, enabling partial soliton recovery. SPM-dominated systems (e.g., ultrafast lasers) exhibit superior noise resilience compared to dispersion-dominated architectures. The derived hyperbolic, elliptic, and singular solutions provide new design principles for noise-resistant optical communication systems. Extending the MEMM to coupled Fokas-Lenells systems with higher-order nonlinearities (e.g., cubic-quintic SPM). Experimental validation of noise-mitigation strategies in fiber-optic setups. This work solidifies the MEMM as a groundbreaking tool for stochastic soliton research, bridging theoretical mathematics and applied photonics. Its insights pave the way for next-generation optical technologies requiring robustness against environmental noise.

6. Results and discussion

The analytical investigations of the stochastic Fokas-Lenells equation have yielded significant insights into soliton dynamics under the influence of nonlinear dispersion and quadratic-cubic SPM. Key findings can be summarized as follows: the MEMM successfully generated multiple classes of solutions, including dark and singular solutions, exponential-type solutions, periodic wave solutions (both trigonometric and elliptic), Jacobi elliptic function solutions, Weierstrass elliptic solutions, and hyperbolic function solutions. These solutions demonstrate the method's capability to handle complex nonlinear terms while maintaining mathematical consistency. The deterministic case ($\sigma_1 = 0$) showed perfect agreement between analytical and numerical results. Progressive noise introduction ($\sigma_1 = 0.4 \rightarrow 1.2$) revealed amplitude fluctuations up to 40% of initial values, phase randomization beyond ($\sigma_1 = 0.7$), and complete coherence breakdown at ($\sigma_1 = 1.2$). Quadratic-cubic SPM demonstrated stabilizing effects for ($\sigma_1 \leq 0.5$), and nonlinear dispersion prevented wave collapse in high-noise regimes ($\sigma_1 > 0$). SPM-dominated configurations showed 50% better stability than dispersion-dominated cases. These results establish fundamental guidelines for optical system design, particularly in noise-resistant fiber optic communications, ultrafast laser pulse stabilization, and nonlinear waveguide engineering. The comprehensive solution spectrum obtained through MEMM provides a valuable toolkit for addressing various physical scenarios in nonlinear photonics, while the stability analysis offers practical thresholds for system operation under stochastic conditions.

Funding

This research was funded by Taif University, Saudi Arabia, Project No. (TU-DSPP-2024-81).

Author contributions

Ahmed Ramady: Resources, Writing-review & editing; Hamdy M. Ahmed: Validation, Methodology, Writing-review & editing; Khadiga A. Ismail: Resources, Writing-review & editing; Wafaa B. Rabie: Formal analysis, Software, Methodology.

All authors have read and approved the final manuscript.

Acknowledgments

The authors extend their appreciation to Taif University, Saudi Arabia, for supporting this work through Project Number (TU-DSPP-2024-81).

Conflict of interest

The authors declare that there are no conflicts of interest regarding the publication of this paper.

References

[1] Singh P, Senthilnathan K. Evolution of a solitary wave: optical soliton, soliton molecule and soliton crystal. *Discover Applied Sciences*. 2024; 6(9): 464. Available from: https://doi.org/10.1007/s42452-024-06152-1.

[2] Kuriakose VC, Porsezian K. Elements of optical solitons: An overview. *Resonance*. 2010; 15: 643-666. Available from: https://doi.org/10.1007/s12045-010-0048-y.

[3] Karjanto N. Modeling wave packet dynamics and exploring applications: a comprehensive guide to the nonlinear Schrödinger equation. *Mathematics*. 2024; 12(5): 744. Available from: https://doi.org/10.3390/math12050744.

[4] Hussein HH, Ahmed HM, Alexan W. Analytical soliton solutions for cubic-quartic perturbations of the Lakshmanan-Porsezian-Daniel equation using the modified extended tanh function method. *Ain Shams Engineering Journal*. 2024; 15(3): 102513. Available from: https://doi.org/10.1016/j.asej.2023.102513.

[5] Rabie WB, Ahmed HM, Darwish A, Hussein HH. Construction of new solitons and other wave solutions for a concatenation model using modified extended tanh-function method. *Alexandria Engineering Journal*. 2023; 74: 445-451. Available from: https://doi.org/10.1016/j.aej.2023.05.046.

[6] Hasegawa A, Tappert F. Transmission of stationary nonlinear optical pulses in dispersive dielectric fibers. I. Anomalous dispersion. *Applied Physics Letters*. 1973; 23(3): 142-144. Available from: https://doi.org/10.1063/1.1654836.

[7] Mollenauer LF, Stolen RH, Gordon JP. Experimental observation of picosecond pulse narrowing and solitons in optical fibers. *Physical Review Letters*. 1980; 45(13): 1095-1098. Available from: https://doi.org/10.1103/PhysRevLett.45.1095.

[8] Mollenauer LF, Gordon JP. *Solitons in Optical Fibers: Fundamentals and Applications*. Academic Press; 2006.

[9] Samir I, Ahmed HM, Darwish A, Hussein HH. Dynamical behaviors of solitons for NLSE with Kudryashov's sextic power-law of nonlinear refractive index using improved modified extended tanh-function method. *Ain Shams Engineering Journal*. 2024; 15(1): 102267. Available from: https://doi.org/10.1016/j.asej.2023.102267.

[10] Ahmad J, Mustafa Z. Multi soliton solutions and their wave propagation insights to the nonlinear Schrödinger equation via two expansion methods. *Quantum Studies: Mathematics and Foundations*. 2024; 11(2): 245-261. Available from: https://doi.org/10.1007/s40509-023-00314-3.

[11] Ahmed KK, Badra NM, Ahmed HM, Rabie WB. Unveiling optical solitons and other solutions for fourth-order (2 + 1)-dimensional nonlinear Schrödinger equation by modified extended direct algebraic method. *Journal of Optics*. 2024. Available from: https://doi.org/10.1007/s12596-024-01690-8.

[12] Chong A, Wright LG, Wise FW. Ultrafast fiber lasers based on self-similar pulse evolution: a review of current progress. *Reports on Progress in Physics*. 2015; 78(11): 113901. Available from: https://doi.org/10.1088/0034-4885/78/11/113901.

[13] Liu X, Popa D, Akhmediev N. Revealing the transition dynamics from *Q* switching to mode locking in a soliton laser. *Physical Review Letters*. 2019; 123(9): 093901. Available from: https://doi.org/10.1103/PhysRevLett.123.093901.

[14] Mahmood A, Rehman HU. Construction of the optical soliton solutions for Fokas-Lenells equation by unified solver method. *International Journal of Applied and Computational Mathematics*. 2023; 9(5): 94. Available from: https://doi.org/10.1007/s40819-023-01575-7.

[15] Mihalache D. Localized structures in optical media and Bose-Einstein condensates: An overview of recent theoretical and experimental results. *Romanian Reports in Physics*. 2024; 76(2): 402. Available from: https://doi.org/10.59277/RomRepPhys.2024.76.402.

[16] Zhao Y, Huang Q, Gong T, Xu S, Li Z, Malomed BA. Three-dimensional solitons supported by the spin-orbit coupling and Rydberg-Rydberg interactions in PT-symmetric potentials. *Chaos, Solitons & Fractals*. 2024; 187: 115329. Available from: https://doi.org/10.1016/j.chaos.2024.115329.

[17] Rehman HU, Iqbal I, Hashemi MS, Mirzazadeh M, Eslami M. Analysis of cubic-quartic-nonlinear Schrödinger's equation with cubic-quintic-septic-nonic form of self-phase modulation through different techniques. *Optik*. 2023; 287: 171028. Available from: https://doi.org/10.1016/j.ijleo.2023.171028.

[18] Ali F, Jhangeer A, Muddassar M. Comprehensive classification of multistability and Lyapunov exponent with multiple dynamics of nonlinear Schrödinger equation. *Nonlinear Dynamics*. 2024; 113: 10335-10364. Available from: https://doi.org/10.1007/s11071-024-10781-x.

[19] Shabbir S. *Application of CDSPM and Qualitative Analysis for Dynamical Models*. COMSATS University Islamabad Lahore Campus; 2024.

[20] Arshad M, Yasin F, Aldosary SF, Rezazadeh H, Farman M, Hosseinzadeh MA. Rational function solutions of higher-order dispersive cubic-quintic nonlinear Schrödinger dynamical model and its applications in fiber optics. *Mathematical Methods in the Applied Sciences*. 2025; 48(4): 5300-5314. Available from: https://doi.org/10.1002/mma.10604.

[21] Rizvi STR, Shabbir S. Optical soliton solution via complete discrimination system approach along with bifurcation and sensitivity analyses for the Gerjikov-Ivanov equation. *Optik*. 2023; 294: 171456. Available from: https://doi.org/10.1016/j.ijleo.2023.171456.

[22] Akbar MA, Abdullah FA, Khatun MM. An investigation of optical solitons of the fractional cubic-quintic nonlinear pulse propagation model: an analytic approach and the impact of fractional derivative. *Optical and Quantum Electronics*. 2024; 56(1): 58. Available from: https://doi.org/10.1007/s11082-023-05649-0.

[23] Abbas AH, Abdel-Ghani H, Maksymov IS. Classical and quantum physical reservoir computing for onboard artificial intelligence systems: A perspective. *Dynamics*. 2024; 4(3): 643-670. Available from: https://doi.org/10.3390/dynamics4030033.

[24] Čindrak S, Jaurigue L, Lüdge K. Engineering quantum reservoirs through krylov complexity, expressivity and observability. *arXiv:240912079*. 2024. Available from: https://doi.org/10.48550/arXiv.2409.12079.

[25] Dineshkumar C, Hoon Jeong J, Hoon Joo Y. Non-fragile saturation controller for fractional-order permanent magnet synchronous generator with fuzzy quantized mechanism. *International Journal of Adaptive Control and Signal Processing*. 2025; 39(5): 1048-1063. Available from: https://doi.org/10.1002/acs.3991.

[26] Dineshkumar C, Jeong Jae H, Joo Young H. Observer-based fuzzy control for fractional order PMSG wind turbine systems with adaptive quantized-mechanism. *Communications in Nonlinear Science and Numerical Simulation*. 2024; 136: 108087. Available from: https://doi.org/10.1016/j.cnsns.2024.108087.

[27] Elsherbeny AM, Murad MAS, Arnous AH, Biswas A, Moraru L, Yildirim Y. Quiescent optical soliton perturbation for Fokas-Lenells equation with nonlinear chromatic dispersion and generalized quadratic-cubic form of self-phase modulation structure. *Contemporary Mathematics*. 2025; 6(2): 2308-2338. Available from: https://doi.org/10.37256/cm.6220256359.

[28] Dutta R, Saharia GK, Talukdar S, Nandy S. Soliton management for ultrashort pulse: dark and anti-dark solitons of Fokas-Lenells equation with a damping like perturbation and a gauge equivalent spin system. *Optical and Quantum Electronics*. 2025; 57(2): 163. Available from: https://doi.org/10.1007/s11082-025-08038-x.

[29] Rabie WB, Khalil TA, Badra N, Ahmed HM, Mirzazadeh M, Hashemi M. Soliton solutions and other solutions to the (4 + 1)-dimensional Davey-Stewartson-Kadomtsev-Petviashvili equation using modified extended mapping method. *Qualitative Theory of Dynamical Systems*. 2024; 23(2): 87. Available from: https://doi.org/10.1007/s12346-023-00944-3.

[30] Mshary N, Ahmed HM, Rabie WB. Fractional solitons in optical twin-core couplers with Kerr law nonlinearity and local M-derivative using modified extended mapping method. *Fractal and Fractional*. 2024; 8(12): 755. Available from: https://doi.org/10.3390/fractalfract8120755.